Near-field imaging of locally perturbed periodic surfaces

OPEN ACCESS
IOP Publishing
Inverse Problems

Inverse Problems **35** (2019) 114003 (20pp) https://doi.org/10.1088/1361-6420/ab2e8f

Near-field imaging of locally perturbed periodic surfaces

Xiaoli Liu[1] **and Ruming Zhang**[2,3,4]

[1] INRIA Saclay Ile de France/CMAP Ecole Polytechnique, Palaiseau, France
[2] Institute for Applied and Numerical Mathematics, Karlsruhe Institute of Technology, Karlsruhe, Germany

E-mail: xiaoli.liu@inria.fr and ruming.zhang@kit.edu

Received 31 January 2019, revised 17 June 2019
Accepted for publication 2 July 2019
Published 3 October 2019

Abstract

This paper concerns the inverse scattering problem to reconstruct a locally perturbed periodic surface. Different from scattering problems with quasi-periodic incident fields and periodic surfaces, the scattered fields are no longer quasi-periodic. Thus the classical method for quasi-periodic scattering problems no longer works. The method based on the Floquet–Bloch transform provides an efficient numerical algorithm to solve the direct scattering problem, and a possibility to reconstruct both the unknown periodic part and the unknown local perturbation from the near-field data.

By transforming the original scattering problem into one defined in an infinite rectangle, the information of the surface is included in the coefficients. The numerical scheme contains two steps. The first step is to obtain an initial guess from a sampling method. The second step is to reconstruct the surface. As is proved in the paper, for some incident fields, the corresponding scattered fields carry little information of the perturbation. In this case, we use these scattered fields to reconstruct the periodic surface. Then we could apply the data that carries more information of the perturbation to reconstruct the local perturbation. The Newton-CG method is applied to solve the associated optimization problems. Numerical examples are given at the end of this paper to show the efficiency of our numerical method.

[3] Author to whom any correspondence should be addressed.
[4] The work of the second author was supported by Deutsche Forschungsgemeinschaft (DFG) through CRC 1173.

Keywords: inverse scattering problem, locally perturbed periodic surface, sampling method, Newton-CG method, Floquet–Bloch transform

(Some figures may appear in colour only in the online journal)

1. Introduction

In this paper, we introduce a numerical method for the inverse scattering problem from a locally perturbed periodic surface. Both the periodic part and the local perturbation of the surface are unknown. The aim is to reconstruct both of them from the near-field measurement data.

Since the periodic surface is perturbed, the classical framework for the quasi-periodic scattering problems (i.e. quasi-periodic incident fields with periodic domains) no longer works. An efficient way to solve these problems is the Floquet–Bloch transform. With the help of this Fourier-like transform, the original problem, which is defined in a 2D unbounded domain, can be written into a new one defined in a 3D bounded domain. This method has been applied to perturbed periodic structures in [3] and waveguide problems in [7]. For scattering problems with non-periodic incident fields and periodic surfaces, we refer to [11, 12, 14]. For problems with locally perturbed periodic surfaces, see [10, 13]. In the paper [17], a high order numerical method has been proposed based on the Floquet–Bloch transform and this method is used in this paper to produce the measured data.

The work in this paper is an extension of joint work of the second author with *Prof Armin Lechleiter* in [15]. In that paper, the periodic surface is assumed to be known. A numerical method has been proposed to discover both the location and the shape of a local perturbation. The sampling method introduced by Ito *et al* (see [8]) was extended to find out the location, and a Newton-CG method was applied to reconstruct the shape. However, the setting in this paper is more difficult, i.e. the periodic surface is no longer known. Thus we have to find the perturbation on an unknown periodic surface, and also reconstruct both the periodic surface and the perturbation. In this case, the sampling method in [15] does not work any more, which makes the problem much more challenging.

In this paper, we develop a numerical method for the inverse problem. The first task is to find out the location of both the periodic surface and the perturbation. Since the previous sampling method does not work, we apply the algorithm introduced in [16], which is a fast imaging method to reconstruct rough surfaces. The algorithm provides a rough guess of the locally perturbed surface, thus we could estimate the vertical location of the whole surface, and also figure out the location of the perturbation from a relatively large domain. Then we apply the Newton's method to reconstruct the shapes of both the periodic surface and the local perturbation. The reconstruction contains two steps. The first step is to reconstruct the periodic surface. It is proved that for certain incident fields, the measured data does contain very little information of the local perturbation. Thus in this case, the measured scattered field could be adopted to reconstruct the periodic surface. Based on the former approximation of the periodic surface, we apply the method in [15] to recover the local perturbation.

The rest of this paper is organized as follows. In section 2, we recall the mathematical model of the direct scattering problem and the Floquet–Bloch transform based formulation. In section 3, the estimation is considered for the difference between the scattered fields with and without perturbation. The inverse problem is formulated in section 4, and the Fréchet derivative and its adjoint operator are studied. In section 5, we conclude the algorithm for inverse problems, including the sampling method for the initial guess and the iterative method for the further reconstruction. In section 6, we present three numerical results obtained from our algorithm.

2. Direct scattering problem

2.1. Mathematical model

Given a bounded 2π-periodic function ζ, it defines a periodic surface

$$\Gamma := \{(x_1, \zeta(x_1)) : x_1 \in \mathbb{R}\}.$$

Let the function p be a compactly supported perturbation. For simplicity, suppose $\mathrm{supp}(p) \subset (-\pi, \pi) + 2\pi J$, where $J \in \mathbb{Z}$ is an integer. Let $\zeta_p := \zeta + p$ be the perturbed function and define

$$\Gamma_p := \{(x_1, \zeta_p(x_1)) : x_1 \in \mathbb{R}\}.$$

The domain above Γ and above Γ_p are set to be Ω and Ω_p, respectively.

Remark 1. For simplicity, all the theoretical arguments in sections 2–4 are proved in the case that $J = 0$. These results can be easily extended to any $J \in \mathbb{Z}$ with the translation $x \mapsto x - 2\pi J$.

In this paper, we assume that the surface Γ_p is sound-soft. Given an incident field u^i that satisfies $\Delta u^i + k^2 u^i = 0$ in $\mathbb{R}^2$, it propagates onto Γ_p and then generates the scattered field u^s (or equivalently, the total field $u = u^i + u^s$). For the mathematical model we refer to figure 1. First, u satisfies

$$\Delta u + k^2 u = 0 \quad \text{in } \Omega_p. \tag{1}$$

Second, as the surface Γ_p is sound-soft,

$$u = 0 \quad \text{on } \Gamma_p. \tag{2}$$

Moreover, the scattered field u^s is propagating upwards. The upward propagation radiation condition (UPRC) is typically written as a double layer potential, see [5], and an alternative definition was introduced in [2, 1]. Let H be a real number that is larger than $\|\zeta\|_\infty$ and $\|\zeta_p\|_\infty$, then the UPRC is written as

$$u^s(x_1, x_2) = \frac{1}{2\pi} \int_{\mathbb{R}} \mathrm{e}^{\mathrm{i}\xi x_1 + \mathrm{i}\sqrt{k^2 - \xi^2}\,(x_2 - H)} \widehat{u}^s(\xi, H) \mathrm{d}\xi, \quad x_2 \geqslant H,$$

where $\widehat{u}^s(\xi, H)$ is the Fourier transform of $u^s(x_1, H)$. Define the Dirichlet-to-Neumann map T^+ by

$$\left(T^+ \varphi\right)(x_1) = \frac{\mathrm{i}}{2\pi} \int_{\mathbb{R}} \sqrt{k^2 - \xi^2}\, \mathrm{e}^{\mathrm{i}\xi x_1} \widehat{\varphi}(\xi) \mathrm{d}\xi, \quad \varphi = \frac{1}{2\pi} \int_{\mathbb{R}} \mathrm{e}^{\mathrm{i}\xi x_1} \widehat{\varphi}(\xi) \mathrm{d}\xi.$$

Let $\Gamma_H := \{(x_1, H) : x_1 \in \mathbb{R}\}$, then the UPRC is equivalent to

$$\frac{\partial u}{\partial x_2}(x_1, H) = T^+ \left[u|_{\Gamma_H}\right] + f \ \text{ on } \Gamma_H, \text{ where } f = \frac{\partial u^i}{\partial x_2}(x_1, H) - T^+ \left(u^i|_{\Gamma_H}\right). \tag{3}$$

Define the domain $\Omega_H^p := \mathbb{R} \times (-\infty, H) \cap \Omega_p$ and we consider the problem (1)–(3) in a weighted Sobolev space $H_r^1(\Omega_H^p)$, where the space $H_r^1(\Omega_H^p)$ is defined by

$$H_r^1(\Omega_H^p) := \left\{\varphi \in \mathcal{D}'(\Omega_H^p) : (1 + |x|^2)^{r/2} \varphi \in H^1(\Omega_H^p)\right\}. \tag{4}$$

$\widetilde{H}_r^1(\Omega_H^p)$ is the subspace of $H_r^1(\Omega_H^p)$ such that all the elements vanish on Γ_p. Similarly, we can define the weighted spaces $H_r^{1/2}(\Gamma_H)$ and $H_r^{-1/2}(\Gamma_H)$. From [1], the operator T^+ is bounded and continuous from $H_r^{1/2}(\Gamma_H)$ to $H_r^{-1/2}(\Gamma_H)$ for all $|r| < 1$.

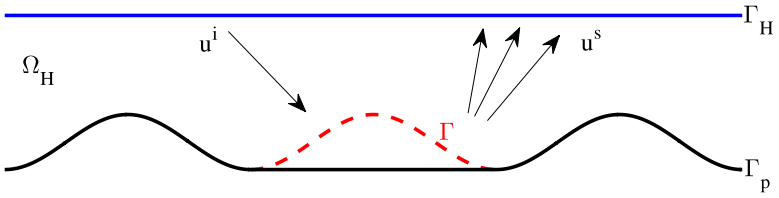

Figure 1. Mathematical model for the scattering problem.

The weak formulation of the scattering problem (1)–(3)is to find $u \in \widetilde{H}_r^1(\Omega_H^p)$ such that

$$\int_{\Omega_H^p} \left[\nabla u \cdot \nabla \overline{v} - k^2 u \overline{v}\right] \mathrm{d}x - \int_{\Gamma_H} T^+ \left(u|_{\Gamma_H}\right) \overline{v} \mathrm{d}s = \int_{\Gamma_H} f \overline{v} \mathrm{d}s \tag{5}$$

for all $v \in \widetilde{H}_r^1(\Omega_H^p)$ with compact support in $\overline{\Omega_H^p}$. The unique solvability of the variational problem (5) has been proved in [1].

Theorem 2. *Given an incident field u^i such that $f \in H_r^{-1/2}(\Gamma_H)$ with $|r| < 1$, then the variational problem (5) has a unique solution $u \in \widetilde{H}_r^1(\Omega_H^p)$.*

Remark 3. Although the unique solvability is proved for bounded surfaces, in this paper, the functions ζ and ζ_p are assumed to be at least Lipschitz continuous.

2.2. Floquet–Bloch transform

During the numerical process of the inverse problem, a Floquet–Bloch transform based numerical method is applied to solve the direct scattering problem. Thus in this section, we give a brief introduction to this method. Let h and H be two real numbers such that $h < \min\{\zeta, \zeta_p\} < \max\{\zeta, \zeta_p\} < H$ and define $D := \mathbb{R} \times (h, H)$. Define the periodic cell W and its dual-cell W^* by

$$W = (-\pi, \pi], \quad W^* = (-1/2, 1/2].$$

Then let $D^{2\pi} = D \cap W \times \mathbb{R}$, $\Gamma_h^{2\pi} = W \times \{h\}$ and $\Gamma_H^{2\pi} = W \times \{H\}$. Define the Bloch transform with period 2π in D by

$$\mathcal{J}_D \varphi(\alpha, x) = \sum_{j \in \mathbb{Z}} \varphi \left(x + \begin{pmatrix} 2\pi j \\ 0 \end{pmatrix}\right) \mathrm{e}^{2\mathrm{i}\pi j \alpha}.$$

The function space $H_0^r(W^*; H_\alpha^s(D^{2\pi}))$ is the closure of $C_0^\infty(W^* \times D^{2\pi})$ with the following norm for $r \in \mathbb{N}$:

$$\|\varphi\|_{H_0^r(W_{\Lambda^*}; H_\alpha^s(D^{2\pi}))} = \left[\sum_{\gamma=0}^{r} \int_{W^*} \|\partial_\alpha^\gamma \psi(\alpha, \cdot)\|_{H_\alpha^s(D^{2\pi})}^2\right]^{1/2}.$$

This definition can be extended to all $r \geqslant 0$ by interpolation between Hilbert spaces and to $r \in \mathbb{R}$ by duality arguments. The following property of the Bloch transform has been investigated in [13].

Theorem 4. *The Bloch transform is an isomorphism between $H_r^s(D)$ and $H_0^r(W^*; H_\alpha^s(D^{2\pi}))$. Further, when $s = r = 0$, $\mathcal{J}_D$ is an isometry with the inverse*

$$(\mathcal{J}_D^{-1}\varphi)\left(x+\begin{pmatrix}2\pi j\\0\end{pmatrix}\right)=\int_{W^*}\varphi(\alpha,x)\mathrm{e}^{2\mathrm{i}\pi j\alpha}\mathrm{d}\alpha,\quad x\in D^{2\pi},\tag{6}$$

and the inverse transform equals to the adjoint operator of $\mathcal{J}_D$.

Now we apply the Floquet–Bloch transform to the scattering problem (5). Following [13], the first task is to transform the original problem, which is defined in the non-periodic domain Ω_H^p, to a problem defined in a periodic domain. In this paper, D is the periodic domain. Let H_0 be a real number that lies in the interval $(\min\{\zeta,\zeta_p\},H)$ and define the following two diffeomorphisms for $x\in\Omega_{H_0}^p$:

$$\Phi_\zeta:x\mapsto\left(x_1,x_2+\frac{(x_2-H_0)^3}{(h-H_0)^3}(\zeta(x_1)-h)\right);\quad \Phi_{\zeta_p}:x\mapsto\left(x_1,x_2+\frac{(x_2-H_0)^3}{(h-H_0)^3}(\zeta_p(x_1)-h)\right).$$

Then extend them by the identity operator for $x_2\geqslant H_0$. As $\mathrm{supp}(\zeta_p-\zeta)\subset W$, $\mathrm{supp}(\Phi_\zeta-\Phi_{\zeta_p})\subset D^{2\pi}$.

Let $u_D=u\circ\Phi_{\zeta_p}$, it can be easily checked that u_D satisfies the following variational equation:

$$\int_D\left[A_{\zeta_p}\nabla u_D\cdot\nabla\overline{v_D}-k^2c_{\zeta_p}u_D\overline{v_D}\right]\mathrm{d}x-\int_{\Gamma_H}T^+\left(u_D\big|_{\Gamma_H}\right)\overline{v_D}\mathrm{d}s=\int_{\Gamma_H}f\overline{v_D}\mathrm{d}s,\tag{7}$$

for all $v_D=v\circ\Phi_{\zeta_p}\in\widetilde{H}^1(D)$, where

$$A_{\zeta_p}(x)=\left|\det\nabla\Phi_{\zeta_p}(x)\right|\left[\left(\nabla\Phi_{\zeta_p}(x)\right)^{-1}\left(\left(\nabla\Phi_{\zeta_p}(x)\right)^{-1}\right)^\top\right]\in L^\infty(D,\mathbb{R}^{2\times2});$$
$$c_{\zeta_p}(x)=\left|\det\nabla\Phi_{\zeta_p}(x)\right|\in L^\infty(D).$$

We define the matrix A_ζ and c_ζ by Φ_ζ in a similar way, i.e.

$$A_\zeta(x)=\left|\det\nabla\Phi_\zeta(x)\right|\left[\left(\nabla\Phi_\zeta(x)\right)^{-1}\left(\left(\nabla\Phi_\zeta(x)\right)^{-1}\right)^\top\right]\in L^\infty(D,\mathbb{R}^{2\times2});$$
$$c_\zeta(x)=\left|\det\nabla\Phi_\zeta(x)\right|\in L^\infty(D).$$

As $\mathrm{supp}(\Phi_\zeta-\Phi_{\zeta_p})\subset D^{2\pi}$, the supports of both $A_{\zeta_p}-A_\zeta$ and $c_{\zeta_p}-c_\zeta$ are subsets of $D^{2\pi}$. Let $w:=\mathcal{J}_Du_D$, then it satisfies

$$\int_{W^*}a_\alpha(w(\alpha,\cdot),z(\alpha,\cdot))\mathrm{d}\alpha+b(\mathcal{J}_\Omega^{-1}w,\mathcal{J}_\Omega^{-1}z)=\int_{W^*}\int_{\Gamma_H^{2\pi}}F(\alpha,\cdot)\overline{z(\alpha,\cdot)}\mathrm{d}\alpha\mathrm{d}s,\tag{8}$$

where

$$a_\alpha(u,v)=\int_{\Omega_H^{2\pi}}\left[A_\zeta\nabla u\cdot\nabla\overline{v}-k^2c_\zeta u\overline{v}\right]\mathrm{d}x-\int_{\Gamma_H^{2\pi}}\left(T_\alpha^+u\right)\overline{v}\mathrm{d}s;$$
$$b(u,v)=\int_{\Omega_H^{2\pi}}\left[(A_{\zeta_p}-A_\zeta)\nabla u\cdot\nabla\overline{v}-k^2(c_{\zeta_p}-c_\zeta)u\overline{v}\right]\mathrm{d}x;$$
$$F(\alpha,\cdot)=\frac{\partial(\mathcal{J}_\Omega u^i)(\alpha,\cdot)}{\partial x_2}-T_\alpha^+(\mathcal{J}_\Omega u^i)(\alpha,\cdot);$$
$$T_\alpha^+\varphi=\mathrm{i}\sum_{j\in\mathbb{Z}}\sqrt{k^2-|j-\alpha|^2}\widehat{\varphi}(j)\mathrm{e}^{\mathrm{i}(j-\alpha)x_1},\ \varphi=\sum_{j\in\mathbb{Z}}\widehat{\varphi}(j)\mathrm{e}^{\mathrm{i}(j-\alpha)x_1}.$$

Following the arguments in [10, 13], it is easy to prove that when the functions ζ and ζ_p are Lipschitz continuous, the variational problem (8) is equivalent to (5). When (5) has a unique solution of $\widetilde{H}^1_r(\Omega^p_H)$ for some $|r| < 1$, the problem (8) has a unique solution in $H^r_0(W^*; \widetilde{H}^1_\alpha(D^{2\pi}))$. Moreover, if the incident field $u^i \in H^2_r(\Omega^p_H)$ and the surfaces are $C^{2,1}$, then the solution belongs to the space $H^r_0(W^*; \widetilde{H}^2_\alpha(D^{2\pi}))$. In [13], a convergent numerical method based on (8) has been proposed for the numerical solution, and a high order method has been proposed in [17].

Remark 5. The information on the periodic function ζ is included in A_ζ and c_ζ, and the information of p is included in A_{ζ_p} and c_{ζ_p}. During the iteration process, when ζ and p are updated, the matrices A_ζ, A_p and the functions c_ζ, c_p are also updated. Thus we do not need to change the meshes during this process.

3. Approximation of the scattering problems with periodic surfaces

This section considers the difference between the scattered fields with and without a local perturbation. Let u_0 be the total field corresponding to the same incident field u^i and periodic surface Γ, then u_0 satisfies the variational equation:

$$\int_{\Omega_H} \left[\nabla u_0 \cdot \nabla \overline{v} - k^2 u_0 \overline{v}\right] \mathrm{d}x - \int_{\Gamma_H} T^+ \left(u_0|_{\Gamma_H}\right) \overline{v} \mathrm{d}s = \int_{\Gamma_H} f \overline{v} \mathrm{d}s.$$

From theorem 2, if $f \in H_r^{-1/2}(\Gamma_H)$ for some $|r| < 1$, then the solution $u_0 \in \widetilde{H}^1_r(\Omega_H)$. In this paper, we assume that $r \in (0, 1)$. As $u_0 \in H^1_r(\Omega_H)$, there exists a constant C that does not depend on u_0 and x_1 such that

$$|u_0(x_1, x_2)| \leqslant C(1 + x_1^2)^{-r/2-1/4}.$$

We apply the translation to the first variable, i.e. to replace x_1 by $x_1 + 2\pi L$ for some $L \in \mathbb{Z} \setminus \{0\}$, and let $u^i_L(x_1, x_2) := u^i(x_1 + 2\pi L, x_2)$ be the incident field. As the surface is 2π-periodic, the total field with the incident field u^i_L, denoted by u^L_0, is actually the function $u_0(x_1 + 2\pi L, x_2)$. u^L_0 satisfies the following variational equation

$$\int_{\Omega_H} \left[\nabla u^L_0 \cdot \nabla \overline{v} - k^2 u^L_0 \overline{v}\right] \mathrm{d}x - \int_{\Gamma_H} T^+ \left(u^L_0|_{\Gamma_H}\right) \overline{v} \mathrm{d}s = \int_{\Gamma_H} f_L \overline{v} \mathrm{d}s$$

with $f_L(x_1, x_2) := f(x_1 + 2\pi L, x_2)$ on Γ_H. As

$$|u_0(x_1 + 2\pi L, x_2)| \leqslant C|2\pi L|^{-r-1/2}, \quad (x_1, x_2) \in \Omega^{2\pi}_H,$$

the following estimate holds:

$$\left|u^L_0(x_1, x_2)\right| \leqslant C|2\pi L|^{-r-1/2}, \quad (x_1, x_2) \in \Omega^{2\pi}_H.$$

Let u^L be the solution of (5) with f replaced by f_L. Similar to the previous section, we can define a diffeomorphism Φ_p that maps Ω^p_H to Ω_H and $\Phi_p - I_2$ is supported in $\Omega_H \cap W \times \mathbb{R}$. Let $u^L_T := u^L \circ \Phi_p$, it is easily checked that u^L_T satisfies

$$\int_{\Omega_H} \left[A_p \nabla u^L_T \cdot \nabla \overline{v} - k^2 c_p u^L_T \overline{v}\right] \mathrm{d}x - \int_{\Gamma_H} T^+ \left(u^L_T|_{\Gamma_H}\right) \overline{v} \mathrm{d}s = \int_{\Gamma_H} f_L \overline{v} \mathrm{d}s, \tag{9}$$

where

$$A_p(x) = |\det \nabla \Phi_p(x)| \left[(\nabla \Phi_p(x))^{-1} \left((\nabla \Phi_p(x))^{-1} \right)^{\top} \right] \in L^{\infty}(D, \mathbb{R}^{2\times 2});$$
$$c_p(x) = |\det \nabla \Phi_p(x)| \in L^{\infty}(D).$$

Moreover, $\mathrm{supp}(A_p - I_2)$, $\mathrm{supp}(c_p - 1) \subset \Omega_H \cap W \times \mathbb{R} (:= \Omega_H^{2\pi})$. Then the difference $u_d^L := u_T^L - u_0^L$ satisfies the following variational equation, i.e.

$$\int_{\Omega_H} \left[A_p \nabla u_d^L \cdot \nabla \overline{v} - k^2 c_p u_d^L \overline{v} \right] - \int_{\Gamma_H} T^+ \left(u_d^L|_{\Gamma_H} \right) \overline{v} \mathrm{d}s = \widetilde{b}(u_0^L, v) \tag{10}$$

for any $v \in H^1(\Omega_H)$ with compact support, where

$$\widetilde{b}(u_0^L, v) = \int_{\Omega_H^{2\pi}} \left[(I_2 - A_p) \nabla u_0^L \cdot \nabla \overline{v} - k^2 (1 - c_p) u_0^L \overline{v} \right] \mathrm{d}x. \tag{11}$$

Here $\widetilde{b}(\cdot, \cdot)$ can be viewed as a bounded sesquilinear form satisfying

$$\left| \widetilde{b}(u, v) \right| \leqslant C \|u\|_{H^1(\Omega_H^{2\pi})} \|v\|_{H^1(\Omega_H^{2\pi})},$$

where C is a constant depending only on ζ and ζ_p. Thus the right hand side of (10) satisfies

$$\left| \widetilde{b}(u_0^L, v) \right| \leqslant C \left\| u_0^L \right\|_{H^1(\Omega_H^{2\pi})} \|v\|_{H^1(\Omega_H^{2\pi})} \leqslant C |2\pi L|^{-r-1/2} \|v\|_{H^1(\Omega_H)}.$$

From the equivalence between (5) and (7), the equation (10) is uniquely solvable in $H^1(\Omega_H)$ when the right hand side is an antilinear functional on $H^1(\Omega_H)$. Thus

$$\left\| u_T^L - u_0^L \right\|_{H^1(\Omega_H)} \leqslant C |2\pi L|^{-r-1/2}.$$

Based on the above analysis, the total field u_0^L is a good approximation of u_T^L if L is sufficiently large. Particularly, let σ be the noise level of the inverse problem and suppose that $L \in \mathbb{Z}$ has a large enough absolute value such that $C|2\pi L|^{-r-1/2} < \delta$, then u_T^L could be treated as the 'exact solution' of the non-perturbed periodic surface with the incident field u_T^L. Let

$$\widetilde{u}_T^L(x_1, x_2) := u_T^L(x_1 - 2\pi L, x_2),$$

then $\widetilde{u}_T^L$ is a good approximation of u_0. In this case, the solution $\widetilde{u}_T^L$ could be applied to reconstruct the periodic surface in the inverse problem.

4. Inverse problem and the Newton-CG method

The inverse problem is to reconstruct the unknown function ζ_p from the measurement Cauchy data U on a horizontal line Γ_H. Here U is defined as

$$U := (u^s, \partial_\nu u^s)\big|_{\Gamma_H} + \sigma (u^s, \partial_\nu u^s)\big|_{\Gamma_H}, \tag{12}$$

where σ is some noise added to the measurement data.

Further, $\zeta \in C^{2,1}(\mathbb{R})$ is supposed to be a 2π-periodic function and $p \in C^{2,1}(\mathbb{R})$ is supposed to be a function that is compactly supported in $W + 2\pi J$ for some $J \in \mathbb{Z}$.

Remark 6. For the inverse problem, J is an unknown integer and one task is to find out the exact value of J. As explained later, the integer J could be obtained by a sampling method (see [16]). In this section, we treat it as a known one. For any $J \neq 0$, we can simply apply the trans-

lation $x \mapsto x - 2\pi J$ to move the perturbation to the center of the domain. Thus for simplicity, we still assume that $J = 0$ in this section.

Define the spaces

$$X := \{\zeta \in C^{2,1}(\mathbb{R}) : \zeta \text{ is } 2\pi - \text{periodic}\};$$
$$Y := \{p \in C^{2,1}(\mathbb{R}) : \text{supp}(p) \subset W\}.$$

In the following, we assume that $(\zeta, p) \in X \times Y$ and $\zeta_p := \zeta + p$. The inverse problem is to find out $(\zeta, p) \in X \times Y$ such that the near-field Cauchy data corresponding to (ζ, p) is the best approximation of U.

4.1. Scattering operator and its properties with respect to rough surfaces

We recall the inverse scattering problems from rough surfaces introduced in [4]. Let $BC^{1,1}(\mathbb{R})$ be the space of bounded, Lipschitz continuous function. Suppose $f \in BC^{1,1}(\mathbb{R})$ and the surface Γ_f is defined by f. We can also define the domain Ω_f by the domain above Γ_f, and Ω_H^f by the domain between Γ_f and Γ_H, where H is a real number that is larger than $\|f\|_\infty$. Given an incident field u^i, we define the following scattering operator

$$\begin{aligned} S: \quad & BC^{1,1}(\mathbb{R}) \to L^2(\Gamma_H) \\ & f \mapsto u^s\big|_{\Gamma_H}. \end{aligned}$$

Then the inverse problem can be written as an optimization problem, i.e. to find $f \in BC^{1,1}(\mathbb{R})$ such that

$$\|S(f) - U\|^2_{L^2(\Gamma_H)} = \min_{f^* \in BC^{1,1}(\mathbb{R})} \|S(f^*) - U\|^2_{L^2(\Gamma_H)}. \tag{13}$$

Let

$$F(f) := \|S(f) - U\|^2_{L^2(\Gamma_H)}, \tag{14}$$

then the inverse problem is to find out the minimizer of the functional F in the domain $BC^{1,1}(\mathbb{R})$. To solve the minimization problem, we have to study the properties of the scattering operator S first.

Theorem 7. *The operator S is differentiable, and its derivative DS is represented as*

$$DS: BC^{1,1}(\mathbb{R}) \to L^2(\Gamma_H) \tag{15}$$
$$h \mapsto u'\big|_{\Gamma_H}, \tag{16}$$

where $u' \in H^1_r(\Omega_H^f)$ *satisfies*

$$\Delta u' + k^2 u' = 0 \quad \text{in } \Omega_H^f; \tag{17}$$

$$u' = -\frac{\partial u}{\partial x_2} h \quad \text{on } \Gamma_f; \tag{18}$$

$$\frac{\partial u'}{\partial x_2} = T^+ u' \quad \text{on } \Gamma_H. \tag{19}$$

Here u is the total field of the scattering problem (1)–(3).

For the proof of this theorem we refer to [4, 9].

In order to use the Newton's method, we also need the adjoint operator of the Fréchet derivative DS, which is explained in the following theorem.

Theorem 8. *The adjoint operator of $DS(f)$, denoted by $[DS(f)]^*$ is given by*

$$[DS(f)]^*\varphi = -\mathrm{Re}\left[\frac{\partial \overline{u}}{\partial \nu}\frac{\partial \overline{z}}{\partial \nu}\right]\nu_2, \tag{20}$$

where ν is the normal derivative upwards, u is the total field and z satisfies

$$\Delta z + k^2 z = 0 \quad \text{in } \Omega_H^f; \tag{21}$$

$$z = 0 \quad \text{on } \Gamma_f; \tag{22}$$

$$\frac{\partial z}{\partial x_2} - T^+ z = \overline{\varphi} \quad \text{on } \Gamma_H. \tag{23}$$

Remark 9. During the iteration steps, the problems (17)–(19) and (21)–(23) will be solved several times. We can always apply the method introduced in section 2.2 to transform the problems first into the one defined in the unbounded rectangle D by the transform Φ_{ζ_p}, and then apply the Floquet–Bloch transform to obtain the new problem defined in the bounded domain $W^* \times D^{2\pi}$. For details of the solution of (21)–(23) we refer to remark 12 in [15].

4.2. Discretization for locally perturbed periodic surfaces

First, the functions ζ and p are approximated by the linear combination of linearly independent functions. Let $\{\varphi_1, \varphi_2, \ldots, \varphi_M\}$ be a set of linearly independent functions in the space X and $\{\psi_1, \psi_2, \ldots, \psi_N\}$ be a set of linearly independent functions in the space Y. Define the finite-dimensional subspaces of X and Y by:

$$X_M := \mathrm{span}\{\varphi_1, \ldots, \varphi_M\} \subset X \quad \text{and} \quad Y_N := \mathrm{span}\{\psi_1, \ldots, \psi_N\} \subset Y.$$

For the coefficients $\boldsymbol{C}^M = (c_1^M, \ldots, c_M^M) \in \mathbb{R}^M$ and $\boldsymbol{D}^N = (d_1^N, \ldots, d_N^N) \in \mathbb{R}^N$, then the elements $\zeta_M \in X_M$ and $p_N \in Y_N$ could be written as

$$\zeta_M(t) = \sum_{m=1}^{M} c_m^M \varphi_m(t), \quad p_N(t) = \sum_{n=1}^{N} d_n^N \psi_n(t).$$

For the function $\zeta \in X$, there is a $\boldsymbol{C}^M \in \mathbb{R}^M$ such that ζ_M is the approximation in X_M of ζ. The argument also holds for $p_N \in Y_N$ and $p \in Y$.

Define the operators A and B by

$$\begin{array}{lll} A: \mathbb{R}^M & \to X_M, & B: \mathbb{R}^N \to Y_N \\ \boldsymbol{C}^M & \mapsto \zeta_M; & \boldsymbol{D}^N \mapsto p_N, \end{array}$$

then the operator P can be defined as

$$\begin{aligned} P:\ & \mathbb{R}^M \times \mathbb{R}^N \to L^2(\Gamma_H) \\ & \left(\boldsymbol{C}^M, \boldsymbol{D}^N\right) \mapsto S \circ \left(A(\boldsymbol{C}^M) + B(\boldsymbol{D}^N)\right), \end{aligned}$$

which maps the coefficients of both the periodic function and the local perturbation to the scattered field. Further, we can define a functional F in the finite dimensional space $\mathbb{R}^M \times \mathbb{R}^N$ by

$$F(\boldsymbol{C}^M, \boldsymbol{D}^N) := \|P(\boldsymbol{C}^M, \boldsymbol{D}^N) - U\|^2_{L^2(\Gamma_H)}. \tag{24}$$

The inverse problem can be reformulated by the following finite dimensional problem:
Discrete inverse problem: find $(\boldsymbol{C}^M, \boldsymbol{D}^N) \in \mathbb{R}^M \times \mathbb{R}^N$ such that

$$F(\boldsymbol{C}^M, \boldsymbol{D}^N) = \min_{(\boldsymbol{C}^M_*, \boldsymbol{D}^N_*) \in \mathbb{R}^M \times \mathbb{R}^N} F(\boldsymbol{C}^M_*, \boldsymbol{D}^N_*). \tag{25}$$

We apply the Newton-CG method to solve the discretized inverse problem. The linearized equation is

$$P(\boldsymbol{C}^M, \boldsymbol{D}^N) + (DP)(\boldsymbol{C}^M, \boldsymbol{D}^N)(\delta \boldsymbol{C}^M, \delta \boldsymbol{D}^N) = U, \tag{26}$$

where $\delta \boldsymbol{C}^M = (\delta c^M_1, \ldots, \delta c^M_M) \in \mathbb{R}^M$ and $\delta \boldsymbol{D}^N = (\delta d^N_1, \ldots, \delta d^N_N) \in \mathbb{R}^N$, $(DP)(\boldsymbol{C}^M, \boldsymbol{D}^N)$ is the Fréchet derivative of P at $(\boldsymbol{C}^M, \boldsymbol{D}^N)$. Define

$$M_A(C^M)(\delta \boldsymbol{C}^M) := (DP)(\boldsymbol{C}^M, \boldsymbol{D}^N)(\delta \boldsymbol{C}^M, \boldsymbol{0});$$
$$M_B(D^N)(\delta \boldsymbol{D}^N) := (DP)(\boldsymbol{C}^M, \boldsymbol{D}^N)(\boldsymbol{0}, \delta \boldsymbol{D}^N),$$

then the linearized equation is written as

$$P(\boldsymbol{C}^M, \boldsymbol{D}^N) + M_A(\boldsymbol{C}^M)(\delta \boldsymbol{C}^M) + M_B(\boldsymbol{D}^N)(\delta \boldsymbol{D}^N) = U. \tag{27}$$

First, we have to calculate the derivative of P. As an operator defined in the finite dimensional space $\mathbb{R}^M \times \mathbb{R}^N$, from direct calculation,

$$\frac{\partial P}{\partial c^M_m} = (DS)(A(\boldsymbol{C}^M) + B(\boldsymbol{D}^N))\varphi_m; \quad \frac{\partial P}{\partial d^N_n} = (DS)(A(\boldsymbol{C}^M) + B(\boldsymbol{D}^N))\psi_n.$$

Thus

$$M_A(\boldsymbol{C}^M)(\delta \boldsymbol{C}^M) = \sum_{m=1}^M \delta c^M_m \frac{\partial P}{\partial c^M_m} = (DS)(A(\boldsymbol{C}^M) + B(\boldsymbol{D}^N)) \left[\sum_{m=1}^M \delta c^M_m \varphi_m\right];$$
$$M_B(\boldsymbol{D}^N)(\delta \boldsymbol{D}^N) = \sum_{n=1}^N \delta d^N_n \frac{\partial P}{\partial d^N_n} = (DS)(A(\boldsymbol{C}^M) + B(\boldsymbol{D}^N)) \left[\sum_{n=1}^N \delta d^N_n \psi_n\right].$$

Given any $\delta \boldsymbol{C}^M \in \mathbb{R}^M$ and $\varphi \in L^2(\Gamma_H)$,

$$\begin{aligned}\left(\delta \boldsymbol{C}^M, M^*_A(\boldsymbol{C}^M)\varphi\right) &= \left((M_A)(\boldsymbol{C}^M)(\delta \boldsymbol{C}^M), \varphi\right) \\ &= \left((DS)(A(\boldsymbol{C}^M) + B(\boldsymbol{D}^N)) \left[\sum_{m=1}^M \delta c^M_m \varphi_m\right], \varphi\right) \\ &= \sum_{m=1}^M \delta c^M_m \left(\varphi_m, \left[(DS)(A(\boldsymbol{C}^M) + B(\boldsymbol{D}^N))\right]^* \varphi\right).\end{aligned}$$

Let $Q = \left[(DS)(A(\boldsymbol{C}^M) + B(\boldsymbol{D}^N))\right]^*$, then

$$M_A^*(\boldsymbol{C}^M)\varphi = ((\varphi_1, Q\varphi), \ldots, (\varphi_M, Q\varphi)). \tag{28}$$

Similarly, we can also get

$$M_B^*(\boldsymbol{D}^N)\varphi = ((\psi_1, Q\varphi), \ldots, (\psi_N, Q\varphi)). \tag{29}$$

In the numerical implementation, we solve the discrete inverse problem separately, i.e. first fix $\boldsymbol{D}^N$ and solve the minimization problem (25) to find out the solution $\boldsymbol{C}^M$. Then we fix $\boldsymbol{C}^M$ and solve the problem with respect to $\boldsymbol{D}^N$.

To solve the minimization problems we apply the Newton-CG method. To minimize the function $F(\boldsymbol{C}^M, \boldsymbol{D}^N)$ with fixed $\boldsymbol{D}^N$, we apply the following Newton-CG method.

Algorithm 1. Newton-CG method—part I.

Input: Data U; $\varepsilon > 0$; $j = 0$; fixed $\boldsymbol{D}^N \in \mathbb{R}^N$.
Initialization: $\boldsymbol{C}_0^M \in \mathbb{R}^M$.
1: **while** $\|P(\boldsymbol{C}_j^M, \boldsymbol{D}^N) - U\|_{L^2(\Gamma_H)} > \varepsilon_1 \|U\|_{L^2(\Gamma_H)}$ **do**
2: *CGNE* iteration scheme to solve $M_A(\boldsymbol{C}_j^M)(\boldsymbol{H}^M) = U - P(\boldsymbol{C}_j^M, \boldsymbol{D}^N)$
3: $\boldsymbol{C}_{j+1}^M = \boldsymbol{C}_j^M + \boldsymbol{H}^M$;
4: $j = j + 1$;
5: **end while**

Similarly, we can also minimize the function $F(\boldsymbol{C}^M, \boldsymbol{D}^N)$ with fixed $\boldsymbol{C}^M$ by the following algorithm:

Algorithm 2. Newton-CG method—part II.

Input: Data U; $\varepsilon > 0$; $j = 0$; fixed $\boldsymbol{C}^M \in \mathbb{R}^M$.
Initialization: $\boldsymbol{D}_0^N \in \mathbb{R}^N$.
1: **while** $\|P(\boldsymbol{C}^M, \boldsymbol{D}_j^N) - U\|_{L^2(\Gamma_H)} > \varepsilon_2 \|U\|_{L^2(\Gamma_H)}$ **do**
2: *CGNE* iteration scheme to solve $M_B(\boldsymbol{D}_j^N)(\boldsymbol{H}^N) = U - P(\boldsymbol{C}^M, \boldsymbol{D}_j^N)$
3: $\boldsymbol{D}_{j+1}^N = \boldsymbol{D}_j^N + \boldsymbol{H}^N$;
4: $j = j + 1$;
5: **end while**

Note that the method to solve the equations $M_A(\boldsymbol{C}_j^M)(\boldsymbol{H}^M) = U - P(\boldsymbol{C}_j^M, \boldsymbol{D}^N)$ and $M_B(\boldsymbol{D}_j^N)(\boldsymbol{H}^N) = U - P(\boldsymbol{C}^M, \boldsymbol{D}_j^N)$ numerically, we adopt the CGNE iteration algorithm, for details we refer to algorithm 7.1, [6].

In the rest of this paper, we choose nonlinear independent functions in X and Y as follows. For the space X, we use M ($M = 2m + 1$ for some $m \in \mathbb{N}$) trigonometrical functions, i.e.

$$\varphi_0(t) = 1;\ \varphi_j(t) = \cos(jt);\ \varphi_{j+m}(t) = \sin(jt), \quad j = 1, 2, \ldots, m.$$

For the space Y, the quartic spline functions are adopted (see remark 4.1, [18]). For the positive integer N, let $h = 2R/(M+5)$ and $t_j = (j+2)h - R$, then the spline function is defined by $\psi_j(t) = \psi((t - t_j)/h)$ for $j = 1, 2, \ldots, N$, where

$$\psi(t) := \sum_{\ell=0}^{k+1} \frac{(-1)^j}{k!} \binom{k+1}{\ell} \left(t + \frac{k+1}{2} - j\right)_+^k,$$

where $z_+^k = z^k$ for $z \geqslant 0$ and equals to 0 when $z < 0$. The parameters are chosen as $R = 4$ and $k = 4$.

Thus let a vector $\boldsymbol{C}_j^M = \left(c_j^0, c_j^1, \ldots, c_j^m, c_j^{m+1}, \ldots, c_j^{2m}\right)$, the periodic surface is defined by the function

$$\zeta(t) = \sum_{\ell=0}^{M} c_j^\ell \varphi_\ell(t) = c_j^0 + \sum_{\ell=1}^{m} c_j^\ell \cos(\ell t) + \sum_{\ell=1}^{m} c_j^{\ell+m} \sin(\ell t).$$

Similarly, if $\boldsymbol{D}_j^N = \left(d_j^1, d_j^2, \ldots, d_j^N\right)$, the local perturbation is defined by

$$p(t) = \sum_{\ell=1}^{N} d_j^\ell \psi_\ell(t).$$

5. Numerical implementation

5.1. Sampling method

In this section, we use the sampling method introduced in [16] to give an initial guess of the perturbed periodic surface, especially for the first term c_0^0 of $\boldsymbol{C}_0^M$ and the integer J of the perturbation.

Suppose that the location y of an incident point source $u^i(x,y)$ is on a horizontal line $\Gamma_H := \{(x_1, H) : x_1 \in \mathbb{R}\}$ above the surface, we measure the Cauchy data $(u^s, \partial_\nu u^s)$ generated by the point source and the perturbed periodic surface on Γ_H. Here, $\partial_\nu u^s$ denotes the normal derivative of u^s on Γ_H with the direction $(0, 1)$.

With the help of the fundamental solution to the two-dimensional Helmholtz equation given by

$$\Phi_k(x,y) := \frac{\mathrm{i}}{4} H_0^{(1)}(k|x-y|), \quad x \neq y,$$

we introduce the following imaging function

$$I(z) = \int_{\Gamma_H} \left| \int_{\Gamma_H} \left(\partial_{\nu(x)} u^s(x,y) \overline{\Phi_k(x,z)} - u^s(x,y) \partial_{\nu(x)} \overline{\Phi_k(x,z)} \right) \mathrm{d}s(x) \right.$$
$$\left. - \frac{\mathrm{i}}{4\pi} \int_{\mathbb{S}_-} \mathrm{e}^{\mathrm{i}k\hat{x}\cdot(y'-z')} \mathrm{d}s(\hat{x}) \right|^2 \mathrm{d}s(y), \tag{30}$$

where $y' = (y_1, -y_2)$ and $z' = (z_1, -z_2)$. From the analysis in [16], we can expect that the imaging function $I(z)$ takes a large value when $z \in \Gamma_p$ and decays as z is away from Γ_p. In this way, we give an initial guess of the perturbed surface.

In the numerical computation, we choose $2P + 1$ incident point sources which are located at $y_j = (jh_{\mathrm{inc}}, H)$, $j = -P, ..., 0, ...P$, here h_{inc} is a fixed interval between two adjacent points. The measurement line Γ_H is truncated to be $\Gamma_{H,A} := \{x \in \Gamma_H : |x_1| < A\}$ which will be discretized uniformly into $2Q$ subintervals so the step size is $h_{\mathrm{mea}} = A/Q$. In addition, the lower-half circle $\mathbb{S}_-$ in the second integral in (30) will also be uniformly discretized into R grids with the step size $\Delta\theta = \pi/R$. Then for each sampling point z we get the following discrete form of (30)

$$I_A(z) = \sum_{j=-P}^{P} \left| h_{\text{mea}} \sum_{i=0}^{2Q} \left(\partial_{\nu(x)} u^s(x_i, y_j) \overline{\Phi_k(x_i, z)} - u^s(x_i, y_j) \partial_{\nu(x)} \overline{\Phi_k(x_i, z)} \right) \right.$$
$$\left. - \frac{\mathrm{i}\Delta\theta}{4\pi} \sum_{k=0}^{R} \mathrm{e}^{\mathrm{i}kd_k \cdot (y_j' - z')} \right|^2 . \tag{31}$$

Here, the measurement points are denoted by $x_i = (-A + \mathrm{i}h, H)$, $i = 0, 1, ..., 2Q$, and the normal directions are denoted by $d_k = (\sin(-\pi + k\Delta\theta), \cos(-\pi + k\Delta\theta))$, $k = 0, 1, ..., R$.

Suppose the sampling area is a rectangle denoted by $[a, b] \times [c, d]$. We set the numbers of sampling points in x_1-direction and x_2-direction to be M_1 and M_2, respectively. Then by (31), we get the indicator matrix $\{I_A(z_{ij})\}_{M_1 \times M_2}$. For each jth-row of this matrix, we figure out the element with the largest value I_A and denote the corresponding index by $\max_j$. The initial guess for the first term c_0^0 of $\boldsymbol{C}_0^M$ can be deduced by the following formula

$$c_0^0 = c + (d - c) \frac{1}{M_1 M_2} \sum_{j=1}^{j=M_1} \max_j . \tag{32}$$

5.2. Iteration method

From the last subsection, we find out the exact value of the integer J. By translation on the first variable, i.e. to let x_1 be replaced with $x_1 + 2\pi J$, the perturbation is moved to W. Thus we could simply set $J = 0$ in this section. We present the iteration method to reconstruct the periodic function ζ and the compactly supported function p in this section.

From section 3, for an incident field $u^i \in H_r^1(\Omega_H^p)$ with some $r \in (0, 1)$, the measured data U_L with the incident field $u^i(\cdot + 2\pi L, \cdot)$ for $L \in \mathbb{Z} \setminus \{0\}$ could be applied to reconstruct the periodic function ζ. The measured data with incident field u^i, denoted by U_0, is then applied to reconstruct the local perturbation p. So we conclude the algorithm for the inverse scattering problem.

Algorithm 3. Numerical method for the inverse problem.

Input: Cauchy data $(u_j^s, \partial_\nu u_j^s)$ generated by point sources located at x_j;
Given: Domain D, $\mathcal{M}$ is a regular mesh for D.

1. Decide J and c_0^0 from the sampling method. Move the perturbation to the center by $x_1 \mapsto x_1 - 2\pi J$.
   Generate the measured date U_0 and U_L with incident fields $u^i(x_1, x_2)$ and $u^i(x_1 + 2\pi L, x_2)$.
   Set the initial guess: $\boldsymbol{C}_0^M := (c_0^0, 0, \ldots, 0)$, $\boldsymbol{D}_0^N = \boldsymbol{0}$.
2. Solve the minimization problem for the fixed $\boldsymbol{D}_0^N$ by algorithm 1:
   $$F(\boldsymbol{C}^M, \boldsymbol{D}_0^N) = \|P(\boldsymbol{C}^M, \boldsymbol{D}_0^N) - U_L\| \to \min .$$
3. Solving the minimization problem for the fixed $\boldsymbol{C}$ by algorithm 2:
   $$F(\boldsymbol{C}^M, \boldsymbol{D}^N) = \|P(\boldsymbol{C}^M, \boldsymbol{D}^N) - U_0\| \to \min .$$

Then $(\boldsymbol{C}^M, \boldsymbol{D}^N)$ is the final result of the numerical scheme.

6. Numerical results

In this section, we present three examples for our numerical method. We define two different periodic surfaces and local perturbations:

$$\zeta_1(t) = 1.5 + \frac{\sin t}{24} - \frac{\cos 2t}{16};$$

$$\zeta_2(t) = 1.5 + \frac{\cos t}{8};$$

$$\zeta_3(t) = \begin{cases} 1.35, & 2\pi/3 \leqslant |t| \leqslant \pi; \\ 1.65, & |t| \leqslant \pi/3; \\ \text{linear}, & \text{otherwise.} \end{cases}$$

$$p_1(t) = 0.000\,25((t+6\pi)^2 - 9)^3 \sin\left(\frac{\pi(t+3)}{3}\right) \mathcal{X}_{[-3-6\pi,3-6\pi]}(t);$$

$$p_2(t) = -\frac{1+\cos t}{8} \mathcal{X}_{[-3+4\pi,3+4\pi]}(t);$$

$$p_3(t) = \begin{cases} 0, & 2\pi/3 \leqslant |t| \leqslant \pi; \\ -0.3, & |t| \leqslant \pi/3; \\ \text{linear}, & \text{otherwise.} \end{cases}$$

We apply algorithm 3 to the following three examples (see figure 2):

Example 1. The periodic surface Γ is defined by ζ_1 and the local perturbation is defined by p_1.

Example 2. The periodic surface Γ is defined by ζ_2 and the local perturbation is defined by p_2.

Example 3. The periodic surface Γ is defined by ζ_3 and the local perturbation is defined by p_3. Note that in this example, both the periodic surface and the local perturbation are piecewise linear.

For both incident point sources and Herglotz wave functions, the measurement data are collected on $\Gamma_{A,H}$ with $A = 25\pi, H = 3$ and it is divided into $2Q = 1500$ subintervals with the step length $h_{\text{mea}} = \pi/300$. Let u_s be the exact data (either the scattered field or its normal derivative) on $\Gamma_{A,H}$, then the measured data is defined as:

$$U_{\text{meas}} := u_s + \sigma \max(u_s)\text{randn},$$

where $\sigma = 5\%$ is the noise level and randn presents random numbers from the standard normal distribution.

6.1. Sampling method

For the sampling method, we choose the sampling area to be a rectangle as $[-20\pi, 20\pi] \times [1.2, 1.9]$. The number of sampling points in x_1-direction and x_2-direction are set to be $M_1 = 1600$ and $M_2 = 400$, respectively. For the first surface, we put 41 incident point sources at $y_j = (j\pi, 3)$ with $j = -20, -19, \ldots, 20$. For the second and third surfaces, we put 21 incident point sources at $y_j = (2j\pi, 3)$ with $j = -10, -9, \ldots, 10$. The wavenumber is chosen to be $k = 3$ for both examples.

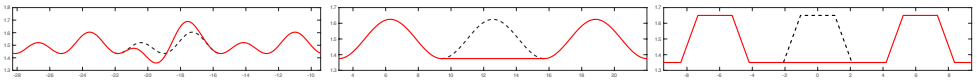

(a) (b) (c)

Figure 2. (a) The first surface; (b) the second surface; (c) the third surface.

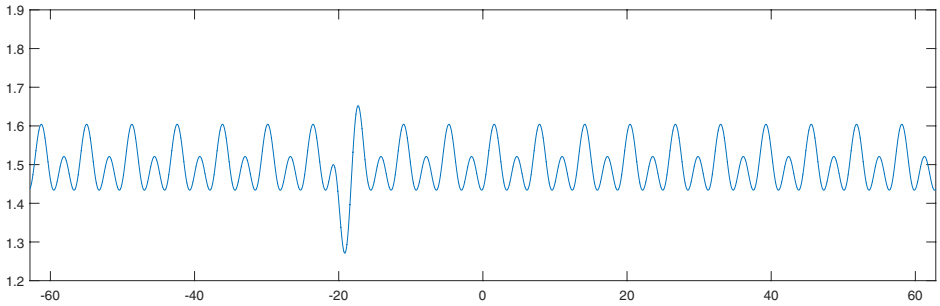

(a)

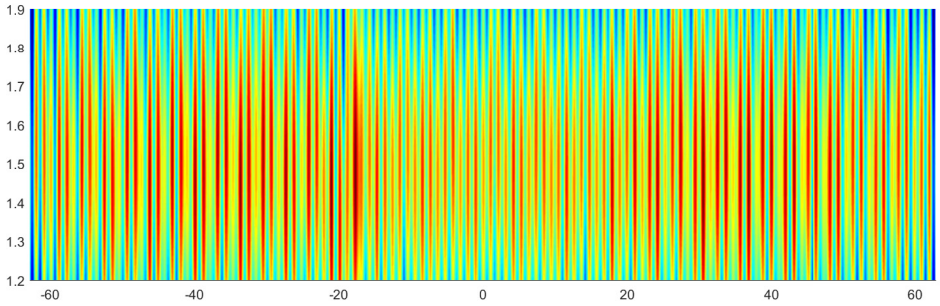

(b)

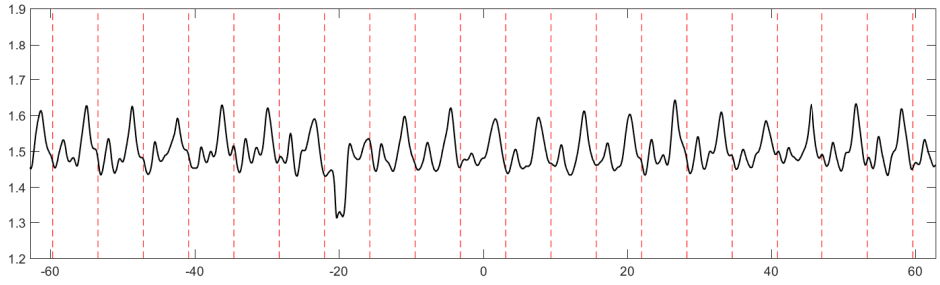

(c)

Figure 3. (a) The first surface; (b) and (c) the reconstructions.

Use the indicator function introduced in (31), we can get a rough reconstruction of the original perturbed periodic surfaces in figures 3 and 4. In each figure, we first present the profile of the original surface. Then the reconstructed result is given directly by the indicator

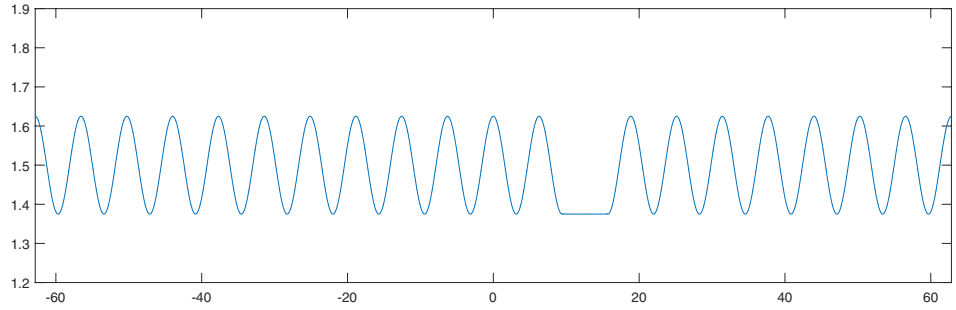

(a)

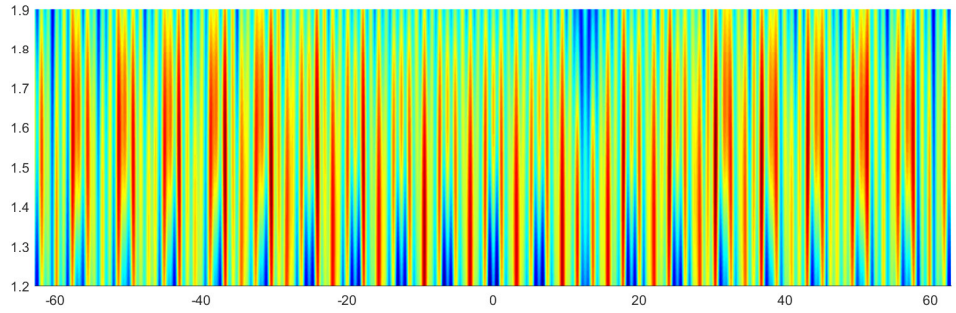

(b)

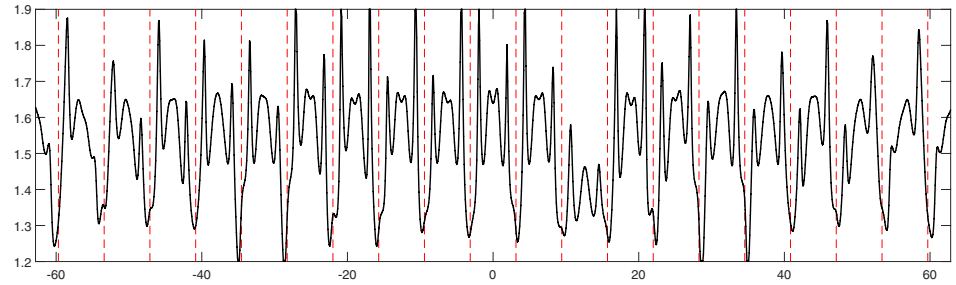

(c)

Figure 4. (a) The first surface; (b) and (c) the reconstructions.

function $I_A(z)$. Finally, in order to give the initail guess of c_0^0 and the integer J of the perturbation, we try to find out the points $z_{\max}$ which get the largest value $I_A(z)$ in each vertical line and plot them in the last position of each figure.

By the end of the sampling step, we determine the values of J and c_0^0. Roughly speaking, J represents the location of the perturbation while c_0^0 gives the vertical location of the periodic surface. From figures 3–5, the locations of the perturbations are easily obtained, i.e. $J = -3$ for example 1, $J = 2$ for example 2 and $J = 0$ for example 3. The initial guess of c_0^0 is computed due to (32). By straightforward calculations, we get $c_0^0 = 1.4987$, $c_0^0 = 1.5216$ and

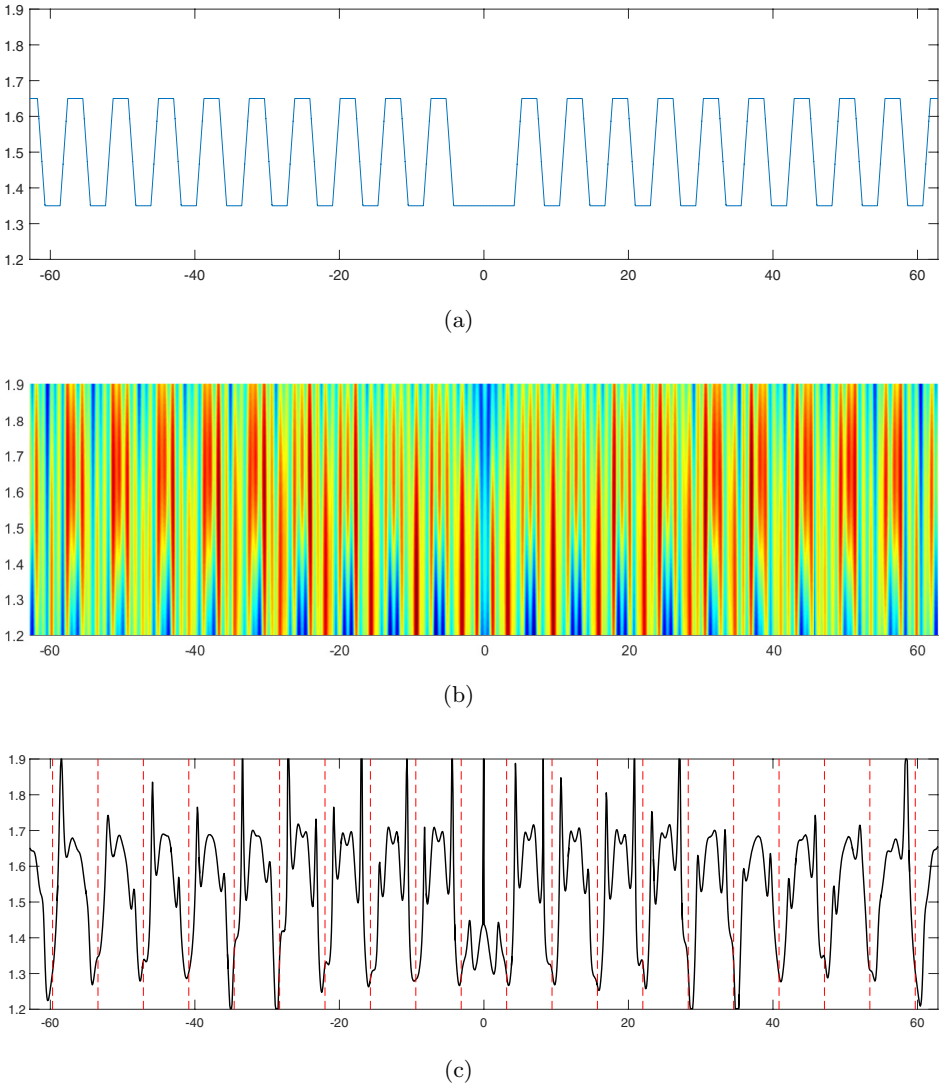

Figure 5. (a) The first surface; (b) and (c) the reconstructions.

$c_0^0 = 1.5296$. All of these two results are very good approximations of the constant terms of ζ_1, ζ_2 and ζ_3.

6.2. Newton's method

For the Newton's method, the Herglotz wave function is applied as the incident field (see figure 6), i.e.

$$u^i(x_1, x_2) = \int_{-\pi/2}^{\pi/2} \exp\left(\mathrm{i}k(x_1 \sin t - x_2 \cos t)\right) g(t)\mathrm{d}t,$$

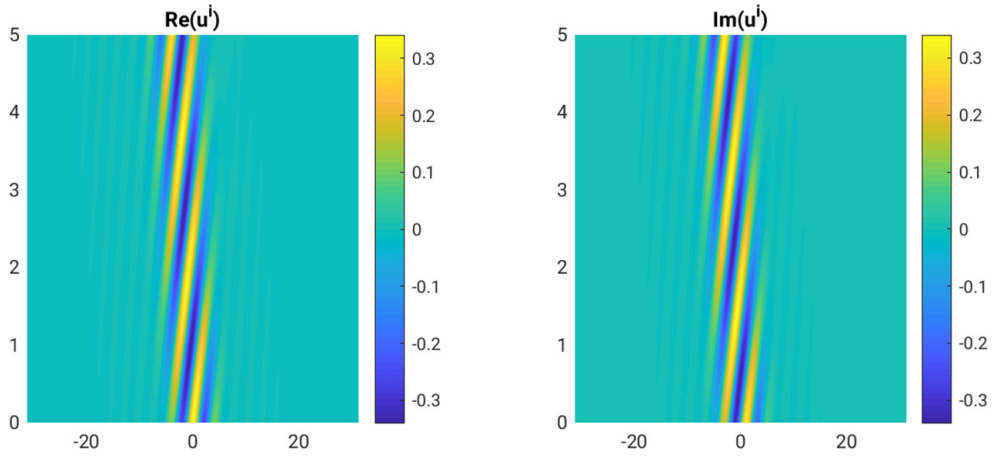

Figure 6. Real- and imaginary-part of the incident field u^i.

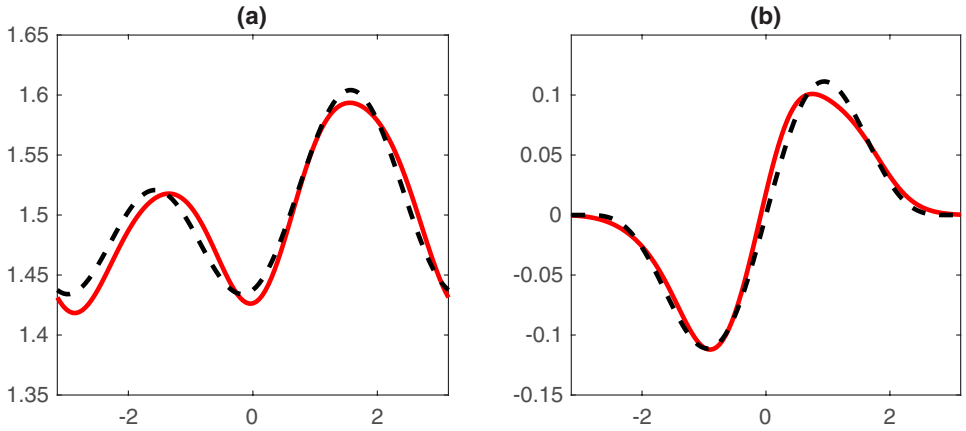

Figure 7. Example 1. Left: reconstruction of ζ_1; right: reconstruction of p_1. Black dotted curves: exact values; red curves: reconstructions.

where

$$g(t) = 2^{12}t^6(1-t)^6\mathcal{X}_{[0,1]}(t).$$

Remark 10. We could not use the point source as the incident fields since the fundamental solution $\Phi(x,y) = \frac{\mathrm{i}}{4}H_0^{(1)}(k|x-y|)$ belongs to the space $H_r^1(\Omega_H^p)$ only if $r < 0$. From [13], the direct solver introduced in section 2.2 does not converge.

The incident field $u^i \in H_r^1(\Omega_H^p)$ for any $r \in (0,1)$. Let $L = 4$, then we use two incident fields u^i and $u_L^i := u^i(\cdot + 2\pi L, \cdot)$. Let u^s and u_L^s be the scattered fields corresponding to the incident fields u^i and u_L^i, and u, u_L be the corresponding total fields. From the estimation in section 3, the error between $u_T^L := u \circ \Phi_p$ and u_0^L, which is the total field with incident field u_L^i and the periodic surface, is bounded by:

$$\left\|u_T^L - u_0^L\right\|_{H^1(\Omega_H)} \leqslant C|8\pi|^{-r-1/2} \leqslant 0.008C.$$

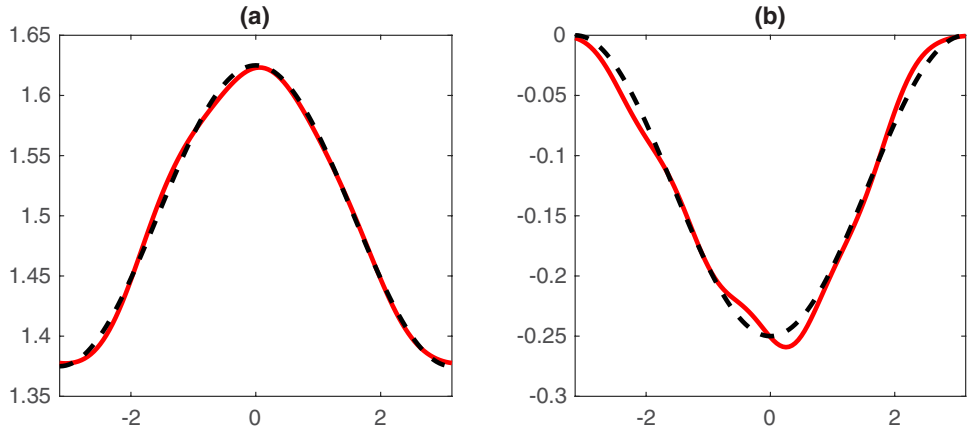

Figure 8. Example 2. Left: reconstruction of ζ_2; right: reconstruction of p_2. Black dotted curves: exact values; red curves: reconstructions.

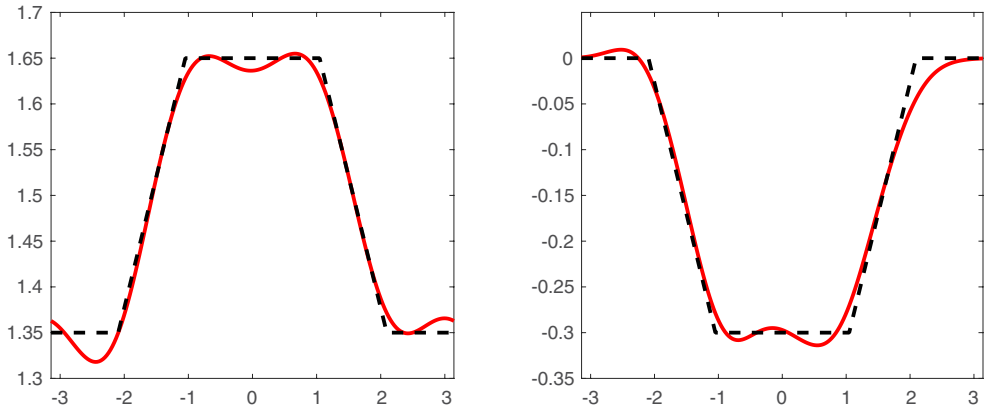

Figure 9. Example 3. Left: reconstruction of ζ_3; right: reconstruction of p_3. Black dotted curves: exact values; red curves: reconstructions.

Note that the noise level is $\sigma = 5\%$, u_T^L could be treated as a good approximation of u_0^L although the constant C is unknown.

The parameters in the Newton-CG algorithm are chosen as follows:

$$h = 1.5,\ M = 9,\ N = 8,\ \varepsilon_1 = 0.05,\ \varepsilon_2 = 0.08.$$

We apply algorithm 3 to reconstruct the perturbation with the known values J and c_0^0 from the sampling method. The reconstructions for examples 1–3 are shown in figures 7–9, respectively. From the left pictures of the three figures, the periodic surfaces are well reconstructed; based on the results for the periodic surfaces, we can also reconstruct the local perturbations very well. However, due to the error from the direct solver, we have to use finer meshes to produce measured data for example 3. Note that as Newton-type methods converge very fast when the initial value is given close enough to a local minimum, a good choice of the initial guess plays an important role in the numerical scheme. With the help of the sampling method, we are able to find a good enough initial guess for the periodic surface. With a good enough approximation of the first element c_0^0 in C_0^M, we have already known the location of

the periodic surface, then Newton-CG method converges when both the periodic surface and the local perturbation have relatively small oscillations.

Acknowledgments

This paper is devoted to Professor Armin Lechleiter. We will never forget him as a talented mathematician, a supportive colleague, and a dear friend.

ORCID iDs

Xiaoli Liu https://orcid.org/0000-0001-8943-3926
Ruming Zhang https://orcid.org/0000-0003-2336-1020

References

[1] Chandler-Wilde S N and Elschner J 2010 Variational approach in weighted Sobolev spaces to scattering by unbounded rough surfaces *SIAM. J. Math. Anal.* **42** 2554–80
[2] Chandler-Wilde S N and Monk P 2005 Existence, uniqueness, and variational methods for scattering by unbounded rough surfaces *SIAM. J. Math. Anal.* **37** 598–618
[3] Coatléven J 2012 Helmholtz equation in periodic media with a line defect *J. Comput. Phys.* **231** 1675–704
[4] Chandler-Wilde S N and Pottast R 2002 The domain derivative in rough-surface scattering and rigorous estimates for first-order perturbation theory *Proc. R. Soc.* A **458** 2967–3001
[5] Chandler-Wilde S N and Zhang B 1998 Electromagnetic scattering by an inhomogeneous conducting or dielectric layer on a perfectly conducting plate *Proc. R. Soc.* A **454** 519–42
[6] Engl H W, Hanke M and Neubauer A 1996 *Regularization of Inverse Problems* (Dordrecht: Kluwer)
[7] Haddar H and Nguyen T P 2016 A volume integral method for solving scattering problems from locally perturbed infinite periodic layers *Appl. Anal.* **96** 130–58
[8] Ito K, Jin B and Zou J 2012 A two-stage method for inverse medium scattering *J. Comput. Phys.* **237** 211–23
[9] Kirsch A 1993 The domain derivative and two applications in inverse scattering theory *Inverse Problems* **9** 81–96
[10] Lechleiter A 2017 The Floquet–Bloch transform and scattering from locally perturbed periodic surfaces *J. Math. Anal. Appl.* **446** 605–27
[11] Lechleiter A and Nguyen D-L 2015 Scattering of Herglotz waves from periodic structures and mapping properties of the Bloch transform *Proc. R. Soc. Edinburgh* A **145** 1283–311
[12] Lechleiter A and Zhang R 2017 A convergent numerical scheme for scattering of aperiodic waves from periodic surfaces based on the Floquet–Bloch transform *SIAM J. Numer. Anal.* **55** 713–36
[13] Lechleiter A and Zhang R 2017 A Floquet–Bloch transform based numerical method for scattering from locally perturbed periodic surfaces *SIAM J. Sci. Comput.* **39** B819–39
[14] Lechleiter A and Zhang R 2017 Non-periodic acoustic and electromagnetic scattering from periodic structures in 3D *Comput. Math. Appl.* **74** 2723–38
[15] Lechleiter A and Zhang R 2018 The reconstruction of a local perturbation in periodic structures *Inverse Problems* **34** 035006
[16] Liu X, Zhang B and Zhang H 2018 A direct imaging method for inverse scattering by unbounded rough surfaces *SIAM J. Imaging Sci.* **11** 1629–50
[17] Zhang R 2018 A high order numerical method for scattering from locally perturbed periodic surfaces *SIAM J. Sci. Comput.* **40** A2286–314
[18] Zhang B and Zhang H 2017 Imaging of locally rough surfaces from intensity-only far-field or near-field data *Inverse Problems* **33** 055001